Enhancement of Coal Fly Ash as a Bleaching Adsorbent for Crude Palm Kernel Oil through Physical and Chemical Activation

Hasnah Ulia [a,1], Hafnimardiyanti [b,2], Agung Kurnia Yahya [a,3], Enny Nurmalasari [a,4,*], Anang Baharudin Sahaq [c,5], Achmad Yanuar Maulana [d,6]

[a] Agro Chemical Engineering Department, ATI Padang Polytechnic, Padang, Indonesia
[b] Chemical Analysis Department, ATI Padang Polytechnic, Padang, Indonesia
[c] Renewable Energy Bioprocess Engineering Department, ATI Padang Polytechnic, Padang, Indonesia
[d] Department of Chemistry, Dong-A University, Busan, South Korea
[1] hasnahulia1@gmail.com; [2] hafnimardiyanti11@gmail.com; [3] agungkurniayahya@gmail.com; [4] ennynurmalasari@poltekatipdg.ac.id*;
[5] anangsahaq92@gmail.com; [6] 1776107@donga.ac.kr
* corresponding author

ARTICLE INFO

Article history
Received April 4, 2026
Revised June 5, 2026
Accepted June 6, 2026

Keywords
Fly Ash
Activation
Bleaching
β -Carotene
Adsorbent

ABSTRACT

Coal fly ash, a major by-product of coal combustion, contains high levels of SiO_2 and Al_2O_3, making it a promising low-cost adsorbent. Despite its widespread use in wastewater treatment, its application as a bleaching adsorbent for crude palm kernel oil (CPKO) remains limited. This study investigates the effectiveness of physically and chemically activated coal fly ash as an alternative adsorbent for CPKO bleaching. Physical activation was performed through calcination at 150 and 300°C, while chemical activation employed 0.5 M phosphoric acid (H_3PO_4) and oxalic acid ($H_2C_2O_4$). Adsorbent dosages ranged from 0.1% to 2.0% (w/v), and all experiments were conducted in triplicate. Two-way ANOVA revealed that both activation method and adsorbent dosage significantly affected residual β-carotene concentration ($p < 0.001$), with a significant interaction between the two factors. Calcination at 300°C increased β-carotene removal from 24.86% to 36.58%, while chemical activation further enhanced adsorption performance. H_3PO_4-activated fly ash achieved the highest β-carotene removal efficiency of 51.22% at a dosage of 0.5%, resulting in the lowest residual β-carotene concentration of 1.44±0.11 ppm. Although commercial bleaching earth provided superior color reduction, activated fly ash produced refined, bleached, and deodorized palm kernel oil (RBDPKO) with acceptable quality, including moisture content below 0.1% and free fatty acid levels of approximately 1.01%, comparable to commercial products. XRD analysis indicated increased crystallinity and $AlPO_4$ formation after phosphoric acid activation, while FTIR confirmed the presence of phosphate functional groups that contributed to enhanced adsorption capacity. These results demonstrate that H_3PO_4-activated coal fly ash is a sustainable and effective alternative adsorbent for palm kernel oil bleaching.

1. Introduction

Coal fly ash is an abundant by-product of coal combustion that contains significant amounts of silica (SiO_2) and alumina (Al_2O_3), making it a promising low-cost adsorbent. Due to its porous structure and surface reactivity, coal fly ash has been widely investigated for adsorption applications, particularly in wastewater treatment and pollutant removal. Previous studies have demonstrated its effectiveness in removing dyes, organic compounds, and heavy metals from aqueous systems, and various activation methods have been employed to enhance its adsorption performance further [1], [2].

To enhance its adsorption performance, coal fly ash has been modified through various physical and chemical activation methods. Treatments with acids and bases, such as HCl and NaOH, have been shown to improve dye removal efficiency significantly, reaching 96.03% for Direct Fast Scarlet 4BS and 93.82% for Direct Sky Blue 5B [3]. Coal fly ash undergoes physical and chemical activation to enhance its adsorption capacity. Thermal treatment removes moisture and volatile compounds, increases pore accessibility, and improves surface properties. Acid activation dissolves impurities, increases the Si/Al ratio, generates new acidic sites, and modifies surface functional groups, thereby enhancing adsorption efficiency. Among activating agents, phosphoric acid (H_3PO_4) promotes pore development and the formation of phosphate-based active sites, while oxalic acid ($H_2C_2O_4$) primarily facilitates selective leaching and complexation of mineral phases [4].

In vegetable oil refining, bleaching is a critical step for removing pigments such as β-carotene, oxidation products, trace metals, and other impurities that degrade oil quality. The adsorption capacity of fly ash is primarily determined by its aluminosilicate composition, which facilitates adsorption via electrostatic interactions, ion exchange, surface complexation, and pore-filling mechanisms. Prior research has demonstrated the successful application of activated fly ash in crude palm oil (CPO) bleaching, indicating its potential as an alternative to commercial bleaching earth.

Despite increasing interest in fly ash-based adsorbents, research on their application in the bleaching of Crude Palm Kernel Oil (CPKO) remains limited. Notably, no systematic comparison has been conducted between phosphoric acid (H_3PO_4) and oxalic acid ($H_2C_2O_4$) activation of coal fly ash for CPKO bleaching. Most existing studies focus on wastewater treatment, heavy-metal adsorption, or CPO bleaching, leaving a significant knowledge gap regarding the effects of different acid activation mechanisms on the adsorption performance of fly ash in CPKO purification. Given this knowledge gap, it is hypothesized that chemical activation with H_3PO_4 and $H_2C_2O_4$ will yield distinct surface characteristics and adsorption performance due to their differing activation mechanisms. Accordingly, the objectives of this study are to evaluate the impact of physical activation (calcination) on the bleaching performance of coal fly ash, compare the effectiveness of H_3PO_4 and $H_2C_2O_4$ as chemical activating agents for coal fly ash, investigate the relationship between the physicochemical characteristics of activated fly ash and its bleaching performance in CPKO, and assess the potential of activated coal fly ash as a sustainable alternative to commercial bleaching earth in CPKO refining. The findings of this study are anticipated to support the development of low-cost, environmentally sustainable adsorbents and to advance the valorization of coal combustion waste for high-value industrial applications.

2. Research Methodology

2.1. Materials

This study used coal fly ash from coal-fired boilers in the palm oil industry as the primary material. The objective was to evaluate its effectiveness as an adsorbent compared with commercial bleaching earth (BE) from a crude palm oil facility in Padang. Chemical reagents, all analytical grade from Merck via PT Medisia Sainsindo, included oxalic acid ($H_2C_2O_4$), phosphoric acid (H_3PO_4), sodium hydroxide (NaOH), ethanol (95%), n-hexane, phenolphthalein indicator, and distilled water. Crude Palm Kernel Oil (CPKO) was used as the feedstock in the bleaching experiments.

2.2. Procedures

1) Sample Preparation and Experimental Design

Coal fly ash was passed through a 200-mesh sieve to achieve a uniform particle size distribution. The resulting material was washed with distilled water to eliminate soluble impurities and subsequently dried in an oven at 100°C for 12 hours until a constant weight was reached. This study employed an experimental design comprising physical and chemical activation treatments. Physical activation was conducted by calcination at 150°C and 300°C, while chemical activation was performed using 0.5 M $H_2C_2O_4$ and 0.5 M H_3PO_4. The bleaching performance of the activated fly ash was evaluated using adsorbent concentrations of 0.1, 0.5, 1.0, 1.5, and 2.0% (w/v). Experiments were conducted in triplicate (n = 3), and results are reported as mean ± standard deviation (SD). Statistical analysis was performed using one-way analysis of variance (ANOVA) at the 95% confidence level to determine differences among treatments. Controlled variables included bleaching temperature (90±2°C), contact time (90 min), stirring speed, and oil volume (100 mL).

2) Physical Activation of Coal Fly Ash

20 grams of fly ash were combined with 100 mL of distilled water and stirred for 10 minutes. The resulting mixture was dried at 100°C and then calcined in a furnace at 150°C and 300°C for 4 hours. Bleaching performance of the physically activated fly ash was assessed by mixing 100 mL of CPKO with fly ash at concentrations of 0.1, 0.5, 1.0, 1.5, and 2.0% (w/v). These mixtures were stirred at 90°C for 90 minutes. The optimum calcination temperature was determined to be the temperature yielding the highest β-carotene removal efficiency [5].

3) Chemical Activation of Coal Fly Ash

The fly ash sample exhibiting the highest performance during physical activation was selected for chemical activation. Twenty grams of calcined fly ash were combined with 100 mL of 0.5 M $H_2C_2O_4$ solution and heated at 100°C for 30 minutes with continuous stirring. After activation, the fly ash was repeatedly washed with distilled water until the wash filtrate reached a neutral pH (6.5–7.0), as measured with a digital pH meter. The neutralized material was then dried at 100°C for 1 hour. The same procedure was applied for activation using 0.5 M H_3PO_4. The chemically activated fly ash samples were subsequently evaluated for CPKO bleaching performance using the procedure described for physical activation.

4) Characterization of Activated Fly Ash

Structural and compositional changes in fly ash resulting from calcination and acid activation were characterized. Crystalline structure and mineral phases were analyzed using X-ray Diffraction (XRD, PANalytical, Netherlands) at 40 kV and 30 mA with Cu-Kα radiation (λ = 1.5406 Å) over a 2θ range of 5–80°. Surface functional groups were identified by Fourier Transform Infrared Spectroscopy (FTIR) within the 400–4000 cm^{-1} wavenumber range. Surface morphology was examined using Scanning Electron Microscopy (SEM, JEOL JSM-6510LV, Japan) at 20 kV and up to 10,000× magnification to assess changes in particle morphology, surface roughness, pore development, and structure following activation [6].

5) Analysis of RBDPKO Quality

The quality of Refined Palm Degummed Kernel Oil (RBDPKO) was evaluated based on free fatty acid (FFA) content, DOBI value, β-carotene concentration, color, and moisture content. The free fatty acid (FFA) content was determined using the alkali titration method. A 5 g sample was placed in an Erlenmeyer flask containing 50 mL of 95% ethanol and heated to boiling to ensure complete dissolution. A few drops of phenolphthalein (PP) indicator were then added, and the hot solution was titrated with a standard NaOH solution until a brick-red endpoint appeared [7]. The FFA value was calculated using Eq. (1).

$$\%\text{FFA} = \frac{V_{\text{titration}} \times N_{\text{NaOH}} \times 25.6}{\text{Sample weight}} \quad (1)$$

The color of CPO was determined according to the AOCS Cc 13b-45 method using a Lovibond Tintometer at 70°C. Measurements were performed using glass cells with a path length of less than 1 inch (25.4 mm) [6]. The color was expressed as Red (R) and Yellow (Y) values obtained from the Tintometer scale. DOBI and β-carotene were analyzed using the UV–Vis spectrophotometric method. A 0.10 g sample was accurately weighed into a 25 mL volumetric flask, dissolved in 95% n-hexane, and filled to the mark. The solution was thoroughly mixed to ensure complete dissolution, and its absorbance spectrum was recorded over the range 200–500 nm using a Shimadzu UV–Vis 1800 Spectrophotometer [7]. The absorbance at 446 nm (A446) was used to determine the β-carotene concentration. In comparison, the absorbances at 446 nm (A446) and 269 nm (A269) were used to calculate the DOBI (Deterioration of Bleachability Index) according to Eqs. (2) and (3).

$$\beta\text{-carotene concentration} = \frac{A_{446} \times 283 \times 25}{\text{Sample weight} \times 100} \quad (2)$$

$$\text{DOBI value} = \frac{A_{446}}{A_{269}} \quad (3)$$

Moisture content was determined gravimetrically. Approximately 5 g of the sample was weighed into a pre-dried crucible and heated at 105°C for 1 hour. After cooling in a desiccator, the crucible was reweighed. The moisture content was calculated using Eq. 4.

$$\text{Moisture Content} = \frac{W_1 - W_2}{W_1} \times 100\% \quad (4)$$

where W1 is the sample weight before drying, and W2 is the weight after drying (g) [8].

3. Results and Discussion

3.1. Evaluation of Coal Fly Ash Performance (Physical–Chemical Activation)

1) Physical Activation

Physical activation is a common method for improving the quality of porous materials, including fly ash, thereby enhancing their effectiveness as adsorbents. This process involves calcination, heating the material at specific temperatures in a furnace without the addition of chemical agents. The purpose of this treatment is to remove moisture, volatile matter, and organic residues while increasing porosity and improving surface structure [9]. In this study, calcination was conducted at 150°C and 300°C, and the performance of fly ash was evaluated based on its ability to reduce β-carotene content in CPKO. The performance results of physically activated fly ash are presented in Fig. 1.

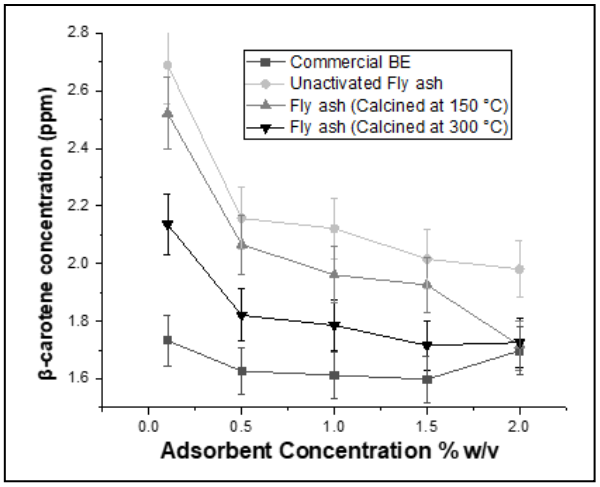

Fig. 1. Performance of Fly Ash After Calcination

Fig. 1 shows the relationship between β-carotene concentration in CPKO and the type of adsorbent used, namely unactivated fly ash, fly ash calcined at 150°C, fly ash calcined at 300°C, and commercial bleaching earth (BE) as a reference. Calcination significantly improved the adsorption capacity of fly ash compared to unactivated fly ash, although its performance remained lower than that of commercial BE typically used in the industry. Previous studies have reported that low-to-moderate temperature calcination (200–300°C) effectively removes volatile compounds and bound water, thereby improving the pore structure of fly ash [10].

Table 1. Statistical validation of adsorbent performance under physical activation

Adsorbent concentration (% w/v)	Type of Adsorbent			
	Commercial BE	***Unactivated Fly ash***	***Fly ash (Calcined at 150°C)***	***Fly ash (Calcined at 300°C)***
0.1	1.73±0.025	2.68±0.045	2.52±0.021	2.13±0.024
0.5	1.62±0.015	2.15±0.032	2.06±0.085	1.82±0.051
1	1.61±0.011	2.12±0.015	1.96±0.058	1.78±0.046
1.5	1.59±0.025	2.01±0.021	1.92±0.023	1.71±0.059
2	1.69±0.052	1.98±0.064	1.71±0.061	1.72±0.006

At adsorbent concentrations ranging from 0.1–0.5% w/v, all adsorbents exhibited a more significant decrease in β-carotene compared to higher concentrations (0.5–2% w/v). At 0.5% w/v, unactivated fly ash reduced β-carotene by only 24.86%, while fly ash calcined at 300°C achieved a higher reduction of 36.58% from the initial concentration of 2.8720±0.156 ppm. Beyond this concentration, the adsorption rate plateaued, indicating that higher adsorbent dosages do not necessarily increase adsorption efficiency [11]. This occurs because, despite an increase in the total number of adsorbed molecules, the overall removal efficiency may decline due to a non-proportional distribution of adsorption sites [12]. Similar behavior was observed in previous studies using Sunflower Seed Shell (SSS) adsorbents, where increasing dosage from 1 g/L to 2.5 g/L raised adsorption efficiency from 66.39% to 89.04%. Still, decreased adsorption capacity (q) from 39.72 to

17.60 mg/g, indicating that excessive adsorbent usage may lower mass-specific effectiveness [13]. From the evaluation results, the optimal fly ash performance in β-carotene adsorption was observed at a concentration of 0.5% w/v. After statistical validation, mean values, error bars, and standard deviations were calculated and are summarized in Table 1. The dataset comprises two factors: adsorbent type and adsorbent concentration. Therefore, a two-way ANOVA analysis was performed, and the results are presented in Table 2.

Table 2. Results of Two-Way ANOVA Analysis

Factor	F	p-value
Type of Adsorbent	450.93	0.0001
Adsorbent concentration	253.93	0.0001
Interaksi	25.57	0.0001

A two-way ANOVA demonstrated that both adsorbent type and concentration significantly affected β-carotene concentration ($p < 0.0001$). A significant interaction was observed, indicating that the effectiveness of fly ash activation depended on the dosage. Commercial bleaching earth resulted in the lowest β-carotene concentration. Among the fly ash samples, fly ash activated at 300°C exhibited superior performance compared to both 150°C-activated and untreated fly ash. The corresponding RBDPKO quality analysis is shown in Table 3.

Table 3. Quality Analysis of RBDPKO at 0.5% w/v Adsorbent Concentration

Parameter	Std. CPKO	Std. RBDPKO	RBDPKO (commercial BE)	RBDPKO (Unactivated fly ash)	RBDPKO Fly ash calcined at 150°C	RBDPKO Fly ash calcined at 300°C
Moisture (%)	0.112 ±0.05	0.1±0.02	0	0.04±0.02	0.05 ± 0.05	0
DOBI Value	0.106 ± 0.05	0.1±0.05	0.035 ±0.01	0.091 ± 0.04	0.088 ±0.05	0.036 ±0.04
FFA (%)	5	1.33	0.987	1.372	1.377	1.148
Color (R/Y)	2.7/18.5	1.1/4.3	2/8.7	2.8/17.7	2.7/17.8	2.7/17.7

Table 3 presents the RBDPKO quality after bleaching with various fly ash types. All samples exhibited very low moisture content (0–0.05%), far below the acceptable limit of <0.5%, indicating good product stability [14]. The DOBI (Deterioration of Bleachability Index) values decreased significantly after bleaching; for instance, fly ash calcined at 300°C had a DOBI of 0.036 (66.03%). This reduction reflects the removal of oxidized pigments and degradation products (decarotenization), confirming the bleaching efficiency [15]. The free fatty acid (FFA) level decreased markedly from 5% in crude CPKO to 0.99–1.38% in bleached RBDPKO, approaching the commercial standard of 1.33%, indicating effective removal of FFA during bleaching. However, the color values (R/Y) of RBDPKO bleached with fly ash (2.7/17.7) remained higher than those obtained with commercial BE (2/8.7), consistent with the β-carotene adsorption performance observed in Fig. 1. Based on the superior performance of fly ash calcined at 300°C, this sample was selected for subsequent chemical activation to enhance its adsorption properties and potential as a BE substitute. Chemical activation aims to increase the pozzolanic reactivity and adsorption capacity of fly ash through acid or base treatments [16]. This process enlarges surface area, enhances porosity, and modifies surface functional groups, making the adsorbent more reactive and efficient [17].

2) Chemical Activation

In this study, two acids were used for activation with H_3PO_4 and $H_2C_2O_4$. Oxalic acid ($H_2C_2O_4$) acts as a reducing and complexing agent, capable of dissolving mineral phases in fly ash and modifying the surface to improve adsorption capacity [18]. Phosphoric acid (H_3PO_4), on the other hand, forms P–O–Si/Al linkages on the surface, leading to phosphate-based geopolymeric structures with high porosity and mechanical stability [12]. The performance of chemically activated fly ash is shown in Fig. 2. Fig. 2 illustrates the bleaching performance of CPKO using different adsorbents, revealing clear differences in β-carotene adsorption efficiency. Among the evaluated materials, fly ash chemically activated with H_3PO_4 consistently demonstrated superior bleaching performance compared to both physically activated fly ash and fly ash activated with $H_2C_2O_4$. The lower average residual β-carotene concentration (1.44±0.11 ppm) obtained with H_3PO_4-activated fly ash indicates a

more effective removal of colored compounds, which can be attributed to enhanced surface acidity, higher pore development, and improved adsorbent–adsorbate interactions resulting from phosphoric acid activation. At an adsorbent dosage of 0.5% (w/v), H_3PO_4 activation achieved a removal efficiency of 51.22%, significantly higher than that of $H_2C_2O_4$ activation (43.89%). This behavior is consistent with previous reports demonstrating the high adsorption capacity of H_3PO_4-activated carbon derived from oil fly ash, including a monolayer adsorption capacity of 196 mg/g for Rhodamine [19].

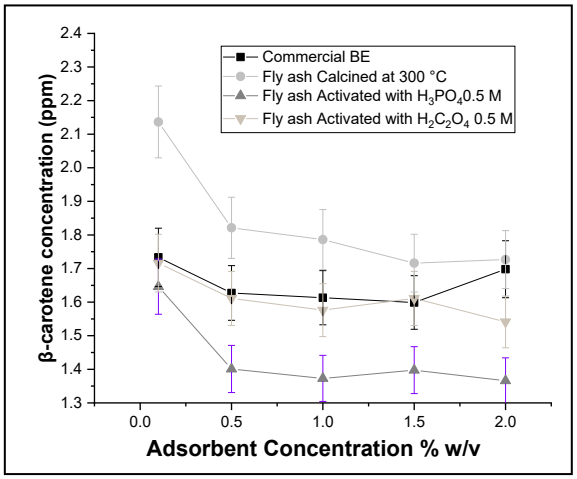

Fig. 2. Performance of Fly Ash After Chemical Activation

H_3PO_4 activation enhances meso- and micropore development, resulting in increased surface area and porosity [20], while the formation of P–O–Si or Al linkages improves structural stability and selectivity toward larger organic molecules in CPKO [21]. In contrast, $H_2C_2O_4$-activated fly ash exhibited comparable initial adsorption performance but reduced stability during the bleaching process. At 0.1% w/v adsorbent concentration, the β-carotene content for $H_2C_2O_4$ activation was 1.715±0.028 ppm, slightly higher than that of H_3PO_4 activation (1.623±0.02 ppm). At 2% w/v, the β-carotene concentration for $H_2C_2O_4$ activation was 1.527±0.001 ppm, still higher than H_3PO_4 activation (1.364±0.004 ppm). This indicates that although oxalic acid may initially enhance surface area and adsorption capacity, its active sites are more susceptible to operational variations than phosphate-treated fly ash [22]. $H_2C_2O_4$ treatment may also induce the formation of oxalate phases that dynamically alter surface composition, yielding good initial adsorption but less stable performance [23].

Table 4. Statistical validation of adsorbent performance under Chemical Activation

Adsorbent concentration (% w/v)	Type of Adsorbent			
	Commercial BE	***Fly ash calcined at 300°C***	***Fly ash Activated with H_3PO_4 0.5M***	***Fly ash Activated with $H_2C_2O_4$ 0.5M***
0.1	1.73±0.025	2.13±0.024	1.64±0.024	1.71±0.028
0.5	1.62±0.015	1.82±0.051	1.40±0.012	1.61±0.004
1	1.61±0.011	1.78±0.046	1.37±0.023	1.57±0.037
1.5	1.59±0.025	1.71±0.059	1.39±0.006	1.61±0.004
2	1.69±0.052	1.72±0.006	1.36±0.004	1.54±0.010

After statistical validation, mean values, error bars, and standard deviations were calculated and are summarized in Table 4. The dataset comprises two factors: adsorbent type and adsorbent concentration. Therefore, two-way ANOVA analysis was performed, and the results are presented in Table 5.

Table 5. Results of Two-Way ANOVA Analysis

Factor	F	p-value
Type of Adsorbent	558.59	1.14×10^{-32}
Adsorbent concentration	172.12	1.24×10^{-24}
Interaksi	15.46	1.99×10^{-11}

A two-way ANOVA (Table 5) showed that both adsorbent type and concentration significantly influenced β-carotene concentration ($F = 558.59$, $p < 0.001$; $F = 172.12$, $p < 0.001$, respectively). A significant interaction was also observed ($F = 15.46$, $p < 0.001$), indicating that each activation method's effectiveness depends on the adsorbent dosage used. The quality of RBDPKO bleached using chemically activated fly ash is presented in Table 2.

Table 6. Quality Analysis of RBDPKO at 0.5% w/v Adsorbent Concentration (Chemical Activation)

Parameter	Stand. RBDPKO	RBDPKO (commercial BE)	RBDPKO (Fly ash calcined at 300°C)	RBDPKO (Fly ash Activated with $H_2C_2O_4$ 0.5 M)	RBDPKO (Fly ash Activated with H_3PO_4 0.5 M)
Moisture (%)	0.1±0.01	0	0	0.1±0.05	0.05±0.01
DOBI Value	0.1067±0.05	0.035±0.052	0.036±0.05	0.119±0.05	0.097±0.051
FFA (%)	1.33	0.987	1.148	1.125	1.010
Color (R/Y)	1.1/4.3	2/8.7	2.7/17.7	2.3/17.6	2.3/16.5

Table 6 shows that all samples had moisture contents below the specified standard, indicating satisfactory hydrolytic stability of the final RBDPKO product. The free fatty acid (FFA) content decreased significantly from approximately 5% in crude CPKO to values near the standard limit, confirming the effectiveness of the bleaching process, especially when using H_3PO_4-activated fly ash. The DOBI value for $H_2C_2O_4$-activated fly ash (0.119) slightly exceeded the standard threshold (0.1067). Despite being marginally above the limit, this result indicates relatively good oil quality with low levels of secondary oxidation products. This deviation is likely due to incomplete removal of oxidized pigments and limited adsorption selectivity. Therefore, this value may be considered borderline acceptable depending on industrial specifications. In contrast, H_3PO_4-activated fly ash achieved a lower DOBI value (0.097), suggesting more efficient removal of oxidation compounds and pigments, likely resulting from the formation of stronger acid sites and improved pore structure.

Color analysis (R/Y) demonstrated that commercial bleaching earth (2/8.7) outperformed H_3PO_4-activated fly ash (2.3/16.5). This finding confirms that although chemical activation enhances fly ash's adsorption performance, it remains less effective than commercial adsorbents at removing pigments, particularly carotenoids. The differences in performance are attributed to several adsorption mechanisms, including electrostatic interactions between surface charge sites and pigment molecules, hydrogen bonding with polar oxidation products, pore-filling effects within mesoporous structures, and weak Lewis acid–base interactions with β-carotene. Nevertheless, the relatively lower surface area and less developed pore network of fly ash, compared to commercial bleaching earth, limit its overall adsorption efficiency.

3.2. Characterization of Fly Ash

The diffraction pattern provides essential information regarding the degree of crystallinity and phase transformations of minerals resulting from calcination and chemical activation processes. XRD characterization was conducted to identify changes in crystalline phases in fly ash after thermal and chemical treatments [5]. Shifts in the diffraction peak positions (2θ) and variations in reflection intensity indicate structural modifications due to interactions between the acids and the mineral constituents of fly ash [24]. The XRD characterization results following physical and chemical activation are presented in Fig. 3.

Fig. 3 presents the XRD patterns of unactivated fly ash, calcined fly ash, and chemically activated fly ash using $H_2C_2O_4$ and H_3PO_4. The dominant diffraction peaks at $2\theta \approx 26.6°$ (quartz) and 33.1°/35.6° (mullite) indicate that the primary crystalline phases in the fly ash consist of SiO_2 and aluminosilicates (Al–Si–O), which are commonly found in coal-derived fly ash [25]. The presence of an amorphous phase, as evidenced by the broad background hump, indicates the formation of glassy aluminosilicate structures during rapid cooling during the combustion process [26]. This amorphous phase is highly reactive and plays a crucial role in activation.

Calcination at 300°C resulted in increased peak intensity and sharpness (from approximately 100 a.u. to 120 a.u.), indicating the removal of physically bound water and surface impurities. Structurally, this suggests that calcination does not significantly alter the primary crystalline phases but enhances structural ordering by eliminating volatile components and improving interparticle contact. This increased structural order is likely to improve the accessibility of active sites on the adsorbent surface.

Chemical activation, particularly with H_3PO_4, led to a further increase in quartz peak intensity and the emergence of additional reflections associated with phosphate-based phases. This behavior indicates a chemical interaction between H_3PO_4 and the aluminosilicate components of the fly ash.

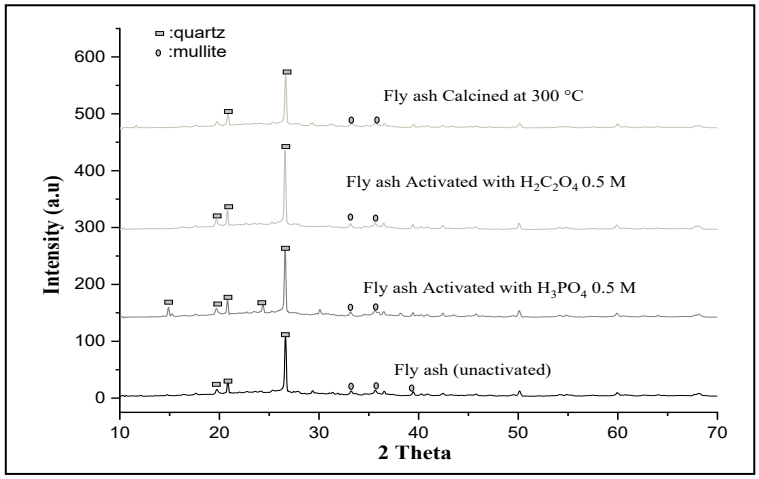

Fig. 3. XRD Characterization of Fly Ash under Various Treatments

Mechanistically, H_3PO_4 can partially dissolve the amorphous aluminosilicate phase, followed by structural reorganization through reactions between Al^{3+} ions and phosphate groups, leading to the formation of phases such as $AlPO_4$. The formation of these phases not only enhances crystallinity but also creates new active sites with higher polarity and acidity, which are essential for the adsorption of colored compounds such as β-carotene [27]. Furthermore, the formation of hydrated phases such as $AlPO_4 \cdot xH_2O$ during activation and subsequent thermal treatment may increase the number of surface hydroxyl groups. These groups act as active centers for adsorption through hydrogen bonding and dipole interactions [28]. This phenomenon explains the correlation between increased crystallinity in H_3PO_4-activated samples and improved adsorption performance during bleaching.

Activation using $H_2C_2O_4$ also increased the crystalline peak intensity to approximately 140 a.u., although this value remained lower than that observed for H_3PO_4 activation (~160 a.u.). This result indicates that both acids induce structural reorganization, albeit through different mechanisms. $H_2C_2O_4$ primarily acts as a selective leaching agent for amorphous phases without inducing the formation of significant new crystalline phases. XRD results confirm that no new crystalline phases were detected after $H_2C_2O_4$ treatment, indicating that the acid modification does not alter the fundamental crystal structure of the fly ash. Quantitative analysis shows a slight increase in the degree of crystallinity, primarily due to the preferential removal of amorphous components rather than the formation of new ordered crystalline structures [23]. Subsequent characterization using Fourier Transform Infrared Spectroscopy (FTIR) was performed to examine the functional group modifications in fly ash that influence its adsorption performance under physical and chemical activation treatments. The FTIR spectra of fly ash samples are presented in Fig. 4.

Fig. 4 compares the FTIR spectra of commercial bleaching earth (bentonite type), unactivated fly ash, and fly ash subjected to calcination and chemical activation. The broad absorption bands observed at ~3400, 2500, and 1620 cm^{-1} in both commercial bentonite and fly ash are attributed to O–H stretching and bending vibrations of adsorbed water (H–O–H). The presence of these bands indicates that the material's surfaces still contain hydroxyl groups and physically adsorbed water, both interacting with the aluminosilicate structure. The bands in the 1000–1100 cm^{-1} region are attributed to asymmetric stretching vibrations of Si–O–Si or Si–O–Al. The persistence of these bands indicates that the fundamental aluminosilicate framework is retained after treatment, suggesting that the modifications primarily occur at the surface rather than by transforming the main structure. After activation with H_3PO_4, new or shifted bands appeared in the 1100–900 cm^{-1} range, which are attributed to P–O, P=O, or bound PO_4 vibrations, consistent with the XRD results. This result indicates that H_3PO_4 interacts with the aluminosilicate components of the fly ash. The decrease in the intensity of O–H bands (~3400 and 1620 cm^{-1}) suggests a reduction in hydroxyl groups, likely due to their interaction with phosphate groups during the activation process [29].

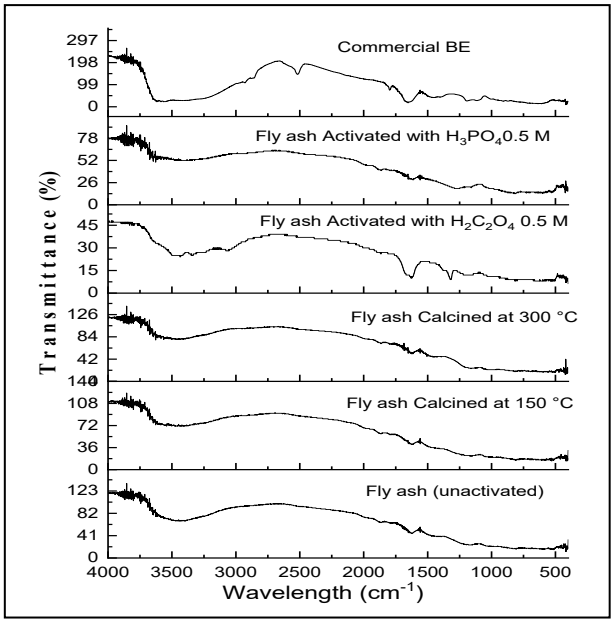

Fig. 4. FTIR Spectra of Fly Ash (Calcined and Chemically Activated)

FTIR analysis was performed to identify functional group modifications in fly ash following calcination and chemical activation. The corresponding absorption bands and their assignments are summarized in Table 7.

Table 7. FTIR peak assignment of fly ash under different treatments

Wavenumber (cm^{-1})	Functional group	Observation (Treatment dependence)
~3400	O–H stretching (hydroxyl, adsorbed water)	Present in all samples; decreased after calcination and acid activation
~1620	H–O–H bending vibration	Present in all samples; reduced intensity after activation
1000–1100	Si–O–Si / Si–O–Al asymmetric stretching	Present in all samples; framework retained
900–1200	P–O / P=O stretching (phosphate groups)	Detected only in H_3PO_4-activated fly ash
1300–1600	O–C–O / metal–oxalate vibrations	Observed in $H_2C_2O_4$-activated fly ash

Activation with $H_2C_2O_4$ results in additional bands at 1300–1600 cm^{-1}, attributed to carbonate vibrations and the formation of metal–oxalate complexes, such as Ca/Fe–oxalate. This observation demonstrates that oxalic acid interacts with surface metal cations, facilitating coordination with surface species and thereby shifting or masking silicate bands and modifying the aluminosilicate environment. Calcination at 150 and 300°C leads to a reduction in O–H bands (~3400 and 1620 cm^{-1}), which is consistent with dehydration and dehydroxylation, as confirmed by XRD analysis showing increased crystallinity. FTIR analysis verifies the structural stability of the aluminosilicate framework, as the Si–O–Si and Si–O–Al bands (1000–1100 cm^{-1}) remain unchanged. Nevertheless, the activation method produces distinct surface modifications. P–O and P=O bands are detected exclusively in H_3PO_4-activated samples, indicating that surface hydroxyl groups react to form Al–O–P and Si–O–P species. These bands are absent in $H_2C_2O_4$-treated samples because oxalic acid does not introduce phosphorus [30]. In contrast, $H_2C_2O_4$ activation produces metal–oxalate and carbonate-related bands, confirming both surface complexation and the leaching of metal ions (Fe^{2+}, Ca^{2+}, Al^{3+}) without heteroatom incorporation. Overall, H_3PO_4 promotes phosphate incorporation and enhances surface acidity, while $H_2C_2O_4$ primarily induces leaching and complexation. These mechanistic differences explain the observed variations in bleaching performance [24]. Morphological changes in fly ash induced by calcination and chemical activation were investigated using scanning electron microscopy (SEM), and the corresponding SEM micrographs are presented in Fig. 5.

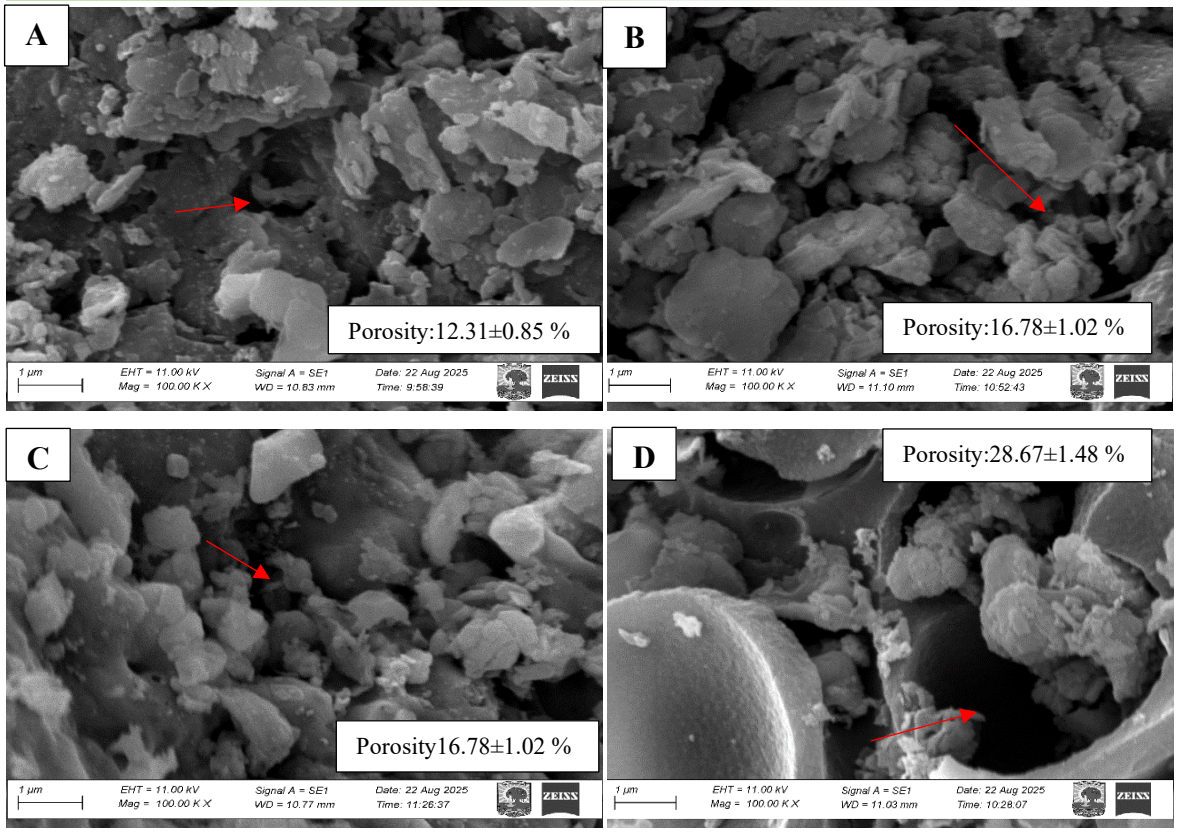

Fig. 5. SEM Results: A) Fly ash without activation, B) Fly ash (Calcined at 300°C), C) Activated with $H_2C_2O_4$, D) Activated with H_3PO_4

Table 8. SEM Results

Sample	Image Parameters			Porosity (%) (Mean±SD)	Notes
	Threshold Method	*Pore Area Fraction (%)*	*Particle Area Fraction (%)*		
A	Otsu	12.31	87.69	12.31±0.85%	Lowest porosity, dominated by dense, compact particles with few visible voids.
B	Otsu	16.78	83.22	16.78±1.02%	Slightly more pores, increased interparticle voids, and microcracks.
C	Otsu	22.45	77.55	16.78±1.02%	Higher porosity, more open structure, and interconnected pores.
D	Otsu	28.67	71.33	28.67±1.48%	Highest porosity, presence of larger voids, and well-developed pore network.

Fig. 5 presents the SEM micrographs of unactivated fly ash, calcined fly ash, and chemically activated fly ash using H_3PO_4 and $H_2C_2O_4$. As shown in Fig. 5A, the unactivated fly ash exhibits a relatively smooth surface with densely agglomerated particles and limited open porosity. This structure indicates that most active surface sites remain covered or are not readily accessible, thereby contributing to reduced adsorption performance.

Calcination at 300°C (Fig. 5B) results in a more open surface, characterized by the formation of small cracks and voids. This change suggests that thermal treatment removes moisture and volatile components that previously covered the surface, thereby opening some pores and improving access to active sites. This observation is consistent with the enhanced adsorption performance compared to unactivated fly ash and is supported by the XRD results, which show sharper diffraction peaks [16]. Chemical activation with $H_2C_2O_4$ (Fig. 5C) and, especially, H_3PO_4 (Fig. 5D) results in a more pronounced increase in surface roughness and porosity. Particle fragmentation, increased intergranular cracking, and the exposure of internal surfaces are clearly observed. These morphological changes indicate that acid activation not only cleans the surface but also induces partial

dissolution of the material, resulting in a more open structure. The difference in the extent of morphological changes between $H_2C_2O_4$ and H_3PO_4 suggests that the type of acid influences the intensity of structural modification. Activation with H_3PO_4 produces a rougher, more developed structure than with $H_2C_2O_4$, indicating a more intensive chemical interaction. This condition increases the specific surface area and the availability of active sites, thereby improving adsorption performance [31].

4. Conclusion

Calcination at 300°C enhanced the adsorption capacity of fly ash, resulting in a β-carotene removal rate of 36.58%. In comparison, H_3PO_4 activation yielded the highest efficiency at 51.22%. H_3PO_4-activated fly ash demonstrated superior bleaching performance among the tested materials; however, the resulting oil color remained less favorable than that produced with commercial bleaching earth. The findings are limited to laboratory-scale experiments. Further research is necessary to assess adsorbent regeneration, conduct a comprehensive techno-economic analysis, and confirm performance in pilot-scale applications.

Acknowledgment

We want to express our sincere gratitude to all parties involved in this research, especially to PT Padang Raya Cakrawala for providing the raw materials, to SMK SMTI Padang for permitting the Lovibond analysis, and to Politeknik ATI Padang for providing the research grant No: B/26/BPSDMI/ATI-Padang/PL/VI/2025.

References

[1] L. Panda and S. Dash, "Characterization and utilization of coal fly ash: A review*," Emerging Materials Research*, vol. 9, no. 3, pp. 921-934, 2020. doi:10.1680/jemmr.18.00097.

[2] M. G. Patel, P. G. Marakana, A. Dey, B. Saini, and H. Chokshi, "Coal fly ash derived adsorbent for enhancing waste water treatment," in *Materials Today: Proceedings*, no. 77, pp.163-167, 2023. doi: 10.1016/j.matpr.2022.11.111.

[3] Z. Hussain, H. Zhang, N. Chang, and H. Wang, "Synthesis of porous materials by the modification of coal fly ash and its environmentally friendly use for the removal of heavy metals from wastewater," *Front. Environ. Sci.*, vol. 10, 2022, doi: 10.3389/fenvs.2022.1085326.

[4] M. Naufa and Azwardi, "Aktivasi Adsorben Fly Ash Batubara Dan Pemanfaatannya Sebagai Pemucat Crude Palm Oil (CPO)," *Jurnal Teknik dan Teknologi*, vol. 13, no. 25, pp.23-28, 2025

[5] A. K. Yahya, E. Nurmalasari, A. P. Aini, and H. N. Ulya, "Performance Evaluation of Bentonite/Nano-SiO2 Composite as Bleaching Earth in Crude Palm Oil Processing," *Jurnal Kimia Sains dan Aplikasi*, vol. 27, no. 4, pp. 167–173, Apr. 2024, doi: 10.14710/jksa.27.4.167-173.

[6] E. Nurmalasari, A. Kurnia Yahya, A. P. Aini, and H. Ulia, "Modification of Bentonite with Nano Silica Oxide (SiO_2) for the Purification Process of Crude Palm Oil (CPO)," *MOTIVECTION: Journal of Mechanical, Electrical and Industrial Engineering*, vol. 7, no. 3, pp. 267-274, 2025, doi: 10.46574/motivection.v7i3.448.

[7] S. Nurulain, N. A. Aziz, M. S. Najib, M. R. Salim, and H. Manap, "A review of free fatty acid determination methods for palm cooking oil," in *Journal of Physics: Conference Series*, vol. 1921, no. 1, 2021. doi: 10.1088/1742-6596/1921/1/012055.

[8] A.K. Yahya, E. Nurmalasari, A.P. Aini, M. Khairati, S. Jung, Z.A.S. Bahlawan, M. Megawati, R. Desiriani, A.Y. Maulana, J. Kim, "Optimization of crude palm oil bleaching process using nano SiO2-bleaching earth: A sustainable approach for enhanced quality and efficiency," *Ind. Crops Prod.*, vol. 239, Jan. 2026, doi: 10.1016/j.indcrop.2025.122525.

[9] T. Ridhowan, E. S. Yusmartini, and D. Kharismadewi, "Optimization of Coal Fly Ash Heating Temperature as an Adsorbent to Improve Acid Mine Water Quality," *Indonesian Journal of Fundamental and Applied Chemistry*, vol. 3, no. 9, pp. 139–146, 2024, doi: 10.24845/ijfac.v9.i3.139.

[10] A. Syarif, Rusdianasari, M. Yerizam, and Sayhirmanyusi, "Characterization of Thermal Activated Fly Ash Adsorbent by Studying the Effect of Temperature," in *Proceedings of the 4th Forum in Research, Science, and Technology (FIRST-T1-T2-2020)*, 2021. doi: 10.2991/ahe.k.210205.015.

[11] M. Khairati, A. Puspita Aini, E. Nurmalasari, and A. Kurnia Yahya, "Comparison of Different Types of Bleaching Earth on the Quality of Bleaching Palm Oil (BPO*)," Eksergi*, vol. 22, no. 1, pp 39-47, 2024. doi: https://doi.org/10.31315/eksergi.v22i1.13311

[12] X. Yang, Y. Wu, Z. Sun, Y. Li, D. Jia, D. Zhang, D. Xiong, M. Wang, "Preparation and Properties of Phosphoric Acid-Based Porous Geopolymer with High Magnesium Nickel Slag and Fly Ash," *Minerals*, vol. 13, no. 4, 2023, doi: 10.3390/min13040564.

[13] B. Hayoun, M. Bourouina, M. Pazos, M. A. Sanromán, and S. Bourouina-Bacha, "Equilibrium study, modeling and optimization of model drug adsorption process by sunflower seed shells," *Applied Sciences (Switzerland)*, vol. 10, no. 9, 2020, doi: 10.3390/app10093271.

[14] R. MacArthur, E. Teye, and S. Darkwa, "Quality and safety evaluation of important parameters in palm oil from major cities in Ghana," *Sci. Afr.*, vol. 13, 2021, doi: 10.1016/j.sciaf.2021.e00860.

[15] A. C. De Jesús-Hernández, R. J. Delgado-Macuil, H. Ruiz-Espinosa, and G. G. Amador-Espejo, "High-power ultrasound bleaching technique for canola oil (Brassica napus L.): Pigments removal and quality parameters," *Food Research International*, vol. 173, 2023, doi: 10.1016/j.foodres.2023.113449.

[16] Fatimah, S. Hardianti, and S. Octaviannus, "Kinerja Aktivasi dan Impregnasi Fly Ash sebagai Adsorben Fenol," *Jurnal Teknik Kimia USU*, vol. 10, no. 2, 2021, doi: 10.32734/jtk.v10i2.5883.

[17] M. Raninga, A. Mudgal, V. K. Patel, J. Patel, and M. Kumar Sinha, "Modification of activated carbon-based adsorbent for removal of industrial dyes and heavy metals: A review," in *Materials Today: Proceedings*, 2023. doi: 10.1016/j.matpr.2022.11.358.

[18] A. I. Arogundade, P. S. M. Megat-Yusoff, F. Ahmad, A. H. Bhat, and L. O. Afolabi, "Modification of bauxite residue with oxalic acid for improved performance in intumescent coatings," *Journal of Materials Research and Technology*, vol. 12, 2021, doi: 10.1016/j.jmrt.2021.03.010.

[19] S. Elamraoui, N. Asdiou, W. Boumya, R. E. Billah, M. El Achaby, N. Barka, E. Lamy, F. E. Alaoui, Y. Chhiti, R. Benhida, M. Achak, "Comparative study of raw Pinus sylvestris sawdust and its activated carbon for chemical oxygen demand and polyphenols removal from Olive Mill Wastewater," *Biomass Convers. Biorefin.*, vol. 15, no. 18, 2025, doi: 10.1007/s13399-025-06814-z.

[20] M. I. Khan, S. Sufian, F. Hassan, R. Shamsuddin, and M. Farooq, "Phosphoric acid based geopolymer foam-activated carbon composite for methylene blue adsorption: isotherm, kinetics, thermodynamics, and machine learning studies," *RSC Adv.*, vol. 15, no. 3, pp. 1989–2010, Jan. 2025, doi: 10.1039/d4ra05782a.

[21] K. Goryunova, Y. Gahramanli, V. Muradkhanli, and P. Nadirov, "Phosphate-activated geopolymers: advantages and application," *RSC advances*, vol. 13, no.43, pp. 30329-30345, 2023. doi: 10.1039/d3ra05131e.

[22] Q. Zeng, S. Wang, L. Hu, H. Zhong, Z. He, W. Sun, D. Xiong, "Oxalic acid modified copper tailings as an efficient adsorbent with super high capacities for the removal of Pb^{2+}," *Chemosphere*, vol. 263, 2021, doi: 10.1016/j.chemosphere.2020.127833.

[23] H. Wu, S. Aruch, R. Grayevsky, Y. Yao, and S. Emmanuel, "Carbon Storage in Coal Fly Ash by Reaction with Oxalic Acid," *ACS ES and T Engineering*, vol. 3, no. 9, 2023, doi: 10.1021/acsestengg.3c00063.

[24] M. Yadav, L. Kumar, V. Yadav, K. Jagannathan, V. N. Singh, S. P. Singh, V. Ezhilselvi, "Optimizing the Fly Ash/Activator Ratio for a Fly Ash-Based Geopolymer through a Study of Microstructure, Thermal Stability, and Electrical Properties," *Ceramics*, vol. 6, no. 4, 2023, doi: 10.3390/ceramics6040144.

[25] S. S. Alterary and N. H. Marei, "Fly ash properties, characterization, and applications: A review," *Journal of King Saud University-Science,* vol. 33, no. 6, 2021. doi: 10.1016/j.jksus.2021.101536.

[26] G. Buema, N. Lupu, H. Chiriac, T. Roman, M. Porcescu, G. Ciobanu, D. V. Burghila, M. Harja, "Eco-Friendly materials obtained by fly ash sulphuric activation for cadmium ions removal," *Materials*, vol. 13, no. 16, 2020, doi: 10.3390/MA13163584.

[27] A. Purbasari, D. Ariyanti, and E. Fitriani, "Adsorption of Methyl Orange Dye by Modified Fly Ash-Based Geopolymer – Characterization, Performance, Kinetics and Isotherm Studies," *Journal of Ecological Engineering*, vol. 24, no. 3, 2023, doi: 10.12911/22998993/157541.

[28] D. Anwar, A. C. E. Putri, K. A. Pramesti, R. B. Cahyono, I. D. Prijambada, and W. Budhijanto, "Optimization of Acid-Catalyzed Hydrolysis of Water Hyacinth without Delignification," *ASEAN Journal of Chemical Engineering*, vol. 25, no. 2, 2025, doi: 10.22146/ajche.21264.

[29] J. A. Park, M. M. Pimenta, and A. C. da S. Bezerra, "Acid Activation in Low-Carbon Binders: A Systematic Literature Review," *Buildings*, vol. 14, no. 1, 2024. doi: 10.3390/buildings14010083.

[30] A. A. Hoyos-Montilla, F. Puertas, J. Molina Mosquera, and J. I. Tobón, "Infrared spectra experimental analyses on alkali-activated fly ash-based binders," *Spectrochim. Acta A Mol. Biomol. Spectrosc.*, vol. 269, 2022, doi: 10.1016/j.saa.2021.120698.

[31] W. R. Wulandari, A. Saefumillah, and R. T. Yunarti, "Modification of fly ash using acids and alkali by hydrothermal method and its application as adsorbents material for phosphate adsorption in aquatic system," in *IOP Conference Series: Materials Science and Engineering*, 2020. doi: 10.1088/1757-899X/902/1/012034.